Experimental hydration of two synthetic glassy blast furnace slags in water and alkaline solutions (NaOH and KOH 0.1 N) at 40° C: structure, composition and origin of the hydrated layer

Z. RAJAOKARIVONY-ANDRIAMBOLOLONA, J. H. THOMASSIN, P. BAILLIF, J. C. TOURAY
Laboratoire de Métallogénie et Géochimie minérale, Ecole Supérieure Energie et Matériaux, Université d'Orléans, 45067 Orléans, France

The hydration of blast furnace slags has been modelled using two synthetic (CaO, SiO$_2$, Al$_2$O$_3$, MgO) glasses with different Al$_2$O$_3$/MgO values. Experiments (duration: 16 h to 150 d) were performed at 40° C in deionized water (pH 6.5) and in NaOH and KOH (0.1 N) solutions (pH = 12.9). The hydrated layer was characterized from a combination of several techniques at different scales: surface analysis by XPS and SEM; TEM of ultrathin diamond-cut sections including electron microdiffraction and EDS analysis; X-ray diffraction of scratched powders. In water, the hydrated zone is only about 0.5 μm thick after 150 d with a leached layer covered by a thin siliceous film on which are scattered rare amorphous lamellae. In alkali media, the hydrated zone is composed of three parts: an inner layer made of modified residual glass, calcium-depleted and richer in magnesium and aluminium than the initial glass; an intermediate lamellar of constant thickness (0.3 μm) after 15 d with magnesium and aluminium as major components ("hydrotalcite type" composition) and labelling the initial solid-solution interface, an outer layer with initially abundant C–S–H more or less carbonated after reaction with atmospheric CO$_2$. The "hydrotalcite-type" layer separates the inner domain dominated by the formation and evolution of a leached glass layer from an outer one, where the precipitation of C–S–H and other amorphous or crystalline compounds, followed by carbonation, are the major processes.

1. Introduction

Blast furnace slags are a by-product of pig-iron production whose composition belongs to the quaternary system SiO$_2$–Al$_2$O$_3$–CaO–MgO, denoted S–A–C–M in cement nomenclature. The technology of their use with Portland cement is well known; concrete made with slag-rich cement, containing 50% to 80% blast furnace slag, has higher resistance to sea-water attack, to alkali-silica reactions and a better development of strengths than Portland cement [1–4].

The mechanisms of slag hydration are not yet well understood although several investigations have been done on the subject [5–12]. In this paper, our investigation concerned the influence of the nature of the solid and aqueous solution on the composition of the hydrated slag and particularly on the magnesium behaviour which is not clear (accumulation at the glass surface). For this study, we have mainly analysed the composition and the structure of the hydrated layer using XPS, electronic microscopy (SEM and TEM with microanalysis EDS and microdiffractions on ultrathin sections) and X-ray diffraction.

2. Experimental details

2.1. Chemical composition of the artificial glasses

Two synthetic glassy slags (L1 and L2) were used. Their chemical compositions are given in Table I. L1 is more aluminous and less magnesian than L2.

2.2. Experiments

The glasses were hydrated in three aqueous media: (i) pure deionized water (pH = 6.5); (ii) two alkaline solutions (NaOH 0.1N and KOH 0.1N with pH = 12.9). Alkaline solution pH was chosen to simulate the pH ($\approx$ 13) of the interstitial solution in the Portland cement.

Experiments were carried out at 40° C, lasting for 4 h to 150 d and the ratio V/SA (V = solution volume, SA = sample area) was about 2 cm. For each run, the solid was a new fresh glass chip, hung on a nylon thread and then dropped into the attack solution. After each reaction, the splinter was rinsed and dried in air.
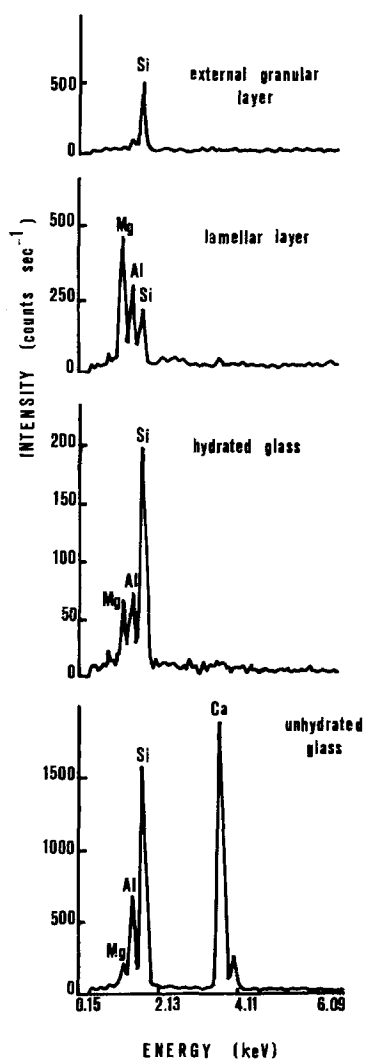
Figure 1 EDS spectra obtained on ultrathin section of L1 slag hydrated in KOH solution for 2 d.

Figure 2 Molar ratio evolution in water (XPS results) for (a) L1 slag and (b) L2 slag. (——) C/S, (– – –) A/S.

2.3. Analytical methods

For our investigations, we used X-ray photoelectron spectroscopy (XPS) to analyse the glass superficial chemical composition, to a depth of about 6 nm [14, 15], SEM to observe the surface morphology, and TEM to study ultrathin sections cut perpendicular to the hydrated layer, using the procedure described by Eberhart and Triki [16]. Thus we have been able to determine the hydrated layer structure and analyse the composition of different hydrated phases using an energy-dispersive X-ray spectroscopy analysis (EDS)
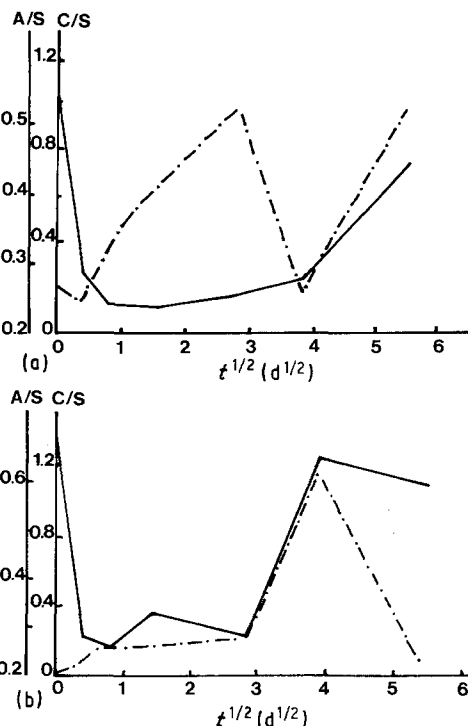
and a calibration scale obtained from ultrathin section analysis of different glasses. The precision may be estimated from a comparison of L1 and L2 composition, determined by EDS and chemical analysis (Table I); Fig. 1 shows selected spectra to illustrate the method. The crystallinity of these phases was investigated by electron microdiffraction.

X-ray diffraction (Debye-Scherrer procedure) was also used for determining the crystallized phases formed after 150 d in alkaline media. For that, the surface deposit was scraped to obtain a powder for X-ray diffraction analysis.

3. Results
3.1. Hydration in deionized water
3.1.1. XPS data

Only aluminium, silicon and calcium have been detected, whereas magnesium is not present on the surface layer. Fig. 2 shows C/S and A/S molar ratios evolution for L1 (Fig. 2a) and for L2 (Fig. 2b). From a general comparison of the curves, two points

TABLE I L1 and L2 slags chemical composition and EDS composition normalized to 100%

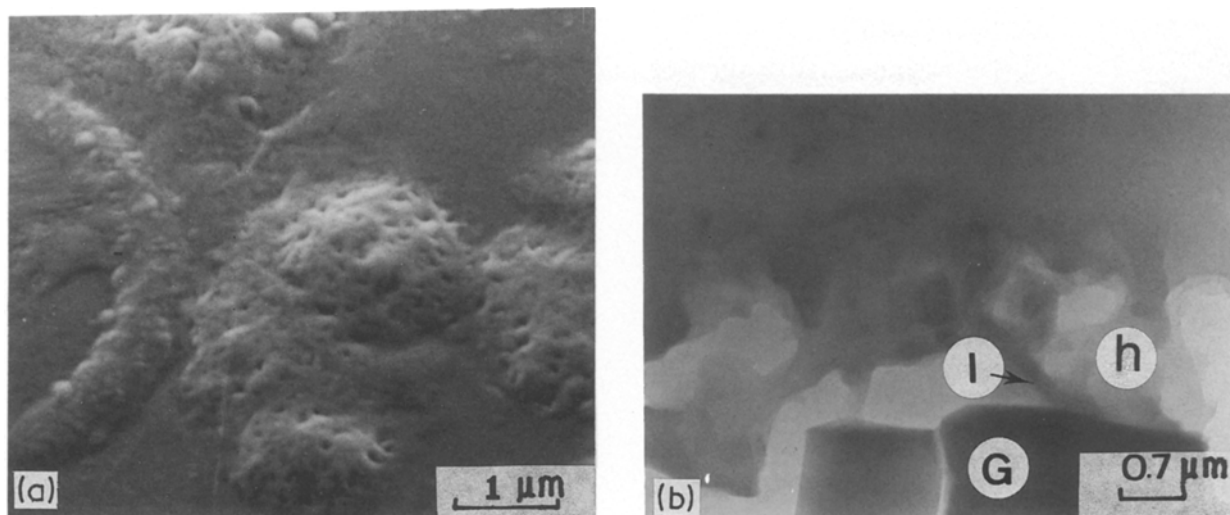| Oxides	L1		L2	
	wt %	EDS composition	wt %	EDS composition
SiO$_2$	33.52	35	33.53	35
Al$_2$O$_3$	15.40	18	12.51	14
CaO	42.71	42	42.11	42
MgO	6.83	5	10.02	9
Fe$_2$O$_3$	0.16	–	1.23	–
Na$_2$O	–	–	0.01	–
K$_2$O	0.02	–	0.13	–
MnO	0.01	–	0.02	–
TiO$_2$	0.23	–	0.17	–
P$_2$O$_5$	0.07	–	–	–
Sulphur	<0.10	–	<0.10	–
Total	98.95	100	99.73	100

Figure 3 L1 slag hydration in water for 150 d (SEM and TEM data). (a) surface morphology and (b) ultrathin section. G = glass; h = hydrated layer; 1 = dark strip.

appeared: (i) calcium is leached from the surface, as soon as the glasses are in contact with the solution, and is later accumulated upon the solid: (ii) aluminium has a more erratic behaviour and may accumulate in an aluminium-bearing phase.

3.1.2. SEM and TEM data

From SEM observations, after 150 d, the L1 surface hydrated layer is formed by a gelatinous phase (Fig. 3a) on which a few calcite crystals have been observed [12]. The L2 surface is covered by globular products (Fig. 4a).

Figs 3b and 4b show ultrathin sections realized on previous samples (TEM data). From the unhydrated glass (G) (appearing dark because of its opacity to electrons), one notices for L1 (Fig. 3b), an hydrated layer (h) composed only by a gelatinous formation including a dark strip (1); and for L2 (Fig. 4b), three distinct zones: (i) a gelatinous layer (H), in contact with the unaltered glass (G), (ii) a lamellar layer, (LL) (iii) an outer globular formation (g1).

The chemical characterization by EDS of the above ultrathin sections is given in Table II. For L1, the

composition of hydrated layer glass (h) is alumino-siliceous, without detectable magnesium and contains a siliceous strip (1); rare scattered amorphous Si-Mg and Si-Al-Mg lamellae have been detected upon these formers. For L2, the hydrated glass (H), is Mg-Al-bearing and more siliceous compared to the unhydrated glass (G). The magnesium enrichment is higher in the lamellar layer (LL) where silicon content has decreased. The globular outer formation (g1) is siliceous. No electron microdiffraction patterns have been obtained, indicating amorphous hydrated products.

The lack of calcium in the hydrated layers at the 0.1 μm scale is not in contradiction with XPS data which indicates a Ca^{2+} adsorption by the Al-Si-rich (for L1) and the Si-rich (for L2) surfaces. Similar results with regard to calcium adsorption on siliceous layers, have been obtained [17-19]. For L1 glass, one notices the lack of magnesium in the hydrated layer (TEM data) as well as on its surface (XPS analysis). For L2 glass, the deep localization of the magnesium-bearing phases explains the lack of magnesium through XPS investigation.

TABLE II Hydration of L1 and L2 in water. TEM and EDS of ultrathin sections of samples after 150 d hydration

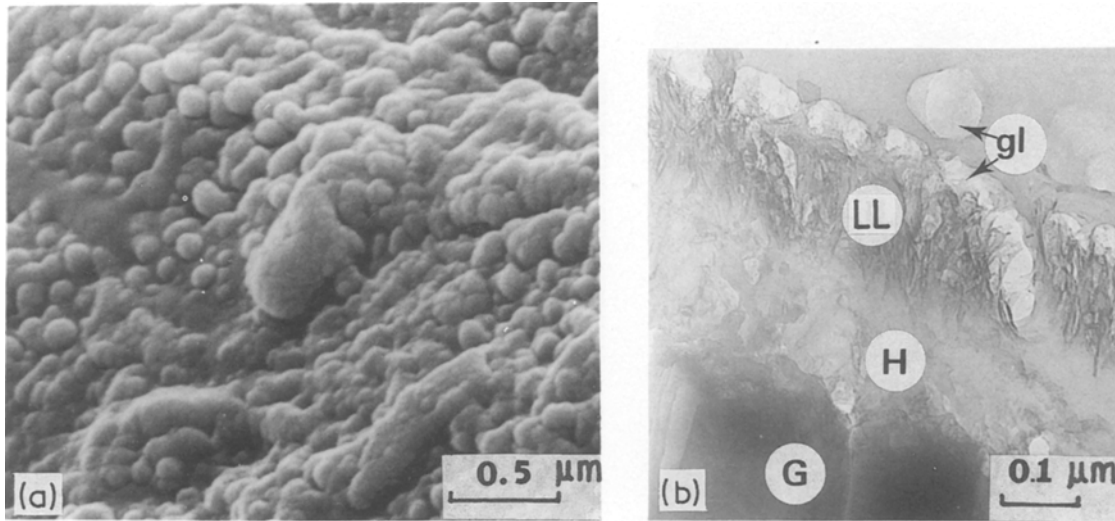| Samples	Chemical composition (wt % oxides)						Morphology
	MgO	Al_2O_3	SiO_2	K_2O	CaO	Fe_2O_3	
L1 150 d (Fig. 3b)	–	44	56	–	–	–	Hydrated (h) layer
	–	–	+ +	–	–	–	Dark (1) strip
	5	18	35	–	42	–	Unhydrated (G) glass
L2 150 d (Fig. 4b)	–	–	+ +	–	–	–	Globules (g1)
	47	25	27	–	–	–	Lamellar (LL) layer
	24	23	53	–	–	–	Hydrated (H) glass
	8	15	34	–	42	–	Unhydrated (G) glass

+ + = abundant.

Figure 4 L2 slag glass hydration in water for 150 d (SEM and TEM data). (a) Surface morphology and (b) ultrathin section. G = glass; H = hydrated glass; LL = lamellar layer; gl = globules.

3.2. Hydration in alkaline media
3.2.1. XPS data for L1 and L2 glasses
Only samples reacted for 30 d have been analysed. Rarely sodium or potassium have been detected at the surface. Molar ratios C/S, A/S and M/S are, respectively, plotted against $t^{1/2}$ (t = hydration time) in Fig. 5 for L1 glass, and in Fig. 6 for L2 glass. The main results are as follows.

For both glasses, calcium on one hand, aluminium and magnesium on the other have opposite behaviour. For L1 glass, the similarity between NaOH curves and KOH curves suggests identical behaviour of the glass in both media. One notices: (i) the development before 16 h of a transient Mg–Al–Si bearing phase, following by (ii) a Ca–Si bearing phase with C/S molar ratios in the 0.8 to 1 range. For L2 glass, different results were observed in both media : (i) the Al–Mg–Si phase has a larger life-time in NaOH than in KOH; (ii) the development of the Ca–Si phase appears more erratic in KOH than in NaOH. In this last medium, the C/S molar ratio is always lower than 0.6.

3.2.2. SEM and TEM data for L1 glass
From SEM observations concerning short runs (2 d), the glass surface morphology (Fig. 7a) appears very similar after reaction in NaOH and KOH solutions. Two types of phase can be easily distinguished: an

internal product (I) formed by scattered lamellae, covered partially by a gelatinous-like "crumpled foil" layer (C). For long runs, in NaOH solution (Fig. 7b), after 150 d, the glass surface is covered by a granular, crackled layer (E) on which a honey-comb formation (F) incorporated dodecahedral particles of hydrogarnet (HG) [12]. After attack in KOH solution, after 105 d (Fig. 7c), the hydrated layer formed on the glass surface is a superposition of a thick layer (1.2 μm) and three thiner ones. Later after 150 d (Fig. 7d), unlike in NaOH solution, abundant thin flake aggregates covered the underlying crackled layer (E); among flakes (f), carbonate crystals are observed [12].

TEM-EDS results, for short hydration times (2 d), in NaOH medium are displayed in Table III. From the unhydrated glass (G) towards the solution, three distinct zones are observed : (i) a granular siliceous layer, forming the hydrated glass (H); (ii) scattered lamellae (L), growing up the previous layer and potassium bearing although only K$^+$ traces (0.02%) were present in the glass. Electron diffraction patterns gave d_{hkl} values compatible with illite structure; (iii) a filamentous layer (C), corresponding to the labelled (C) formation observed on the surface (Fig. 7a). A few magnesium and silicon bearing particles (M = 36%, S = 64%) were scattered in the resin used for making ultrathin sections. These TEM-EDS results are in

Figure 5 Evolution of L1 slag molar ratios in alkaline media. XPS results in (a) NaOH solution and (b) KOH solution . (– – –) M/S, (———) C/S (- - -) A/S.
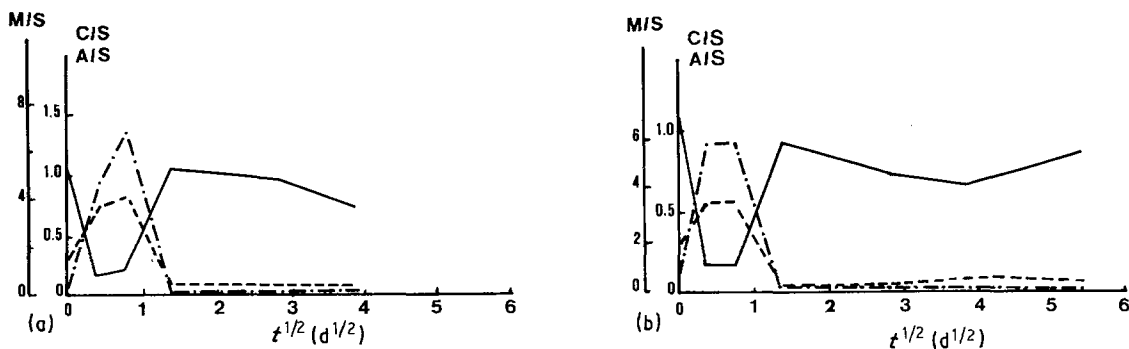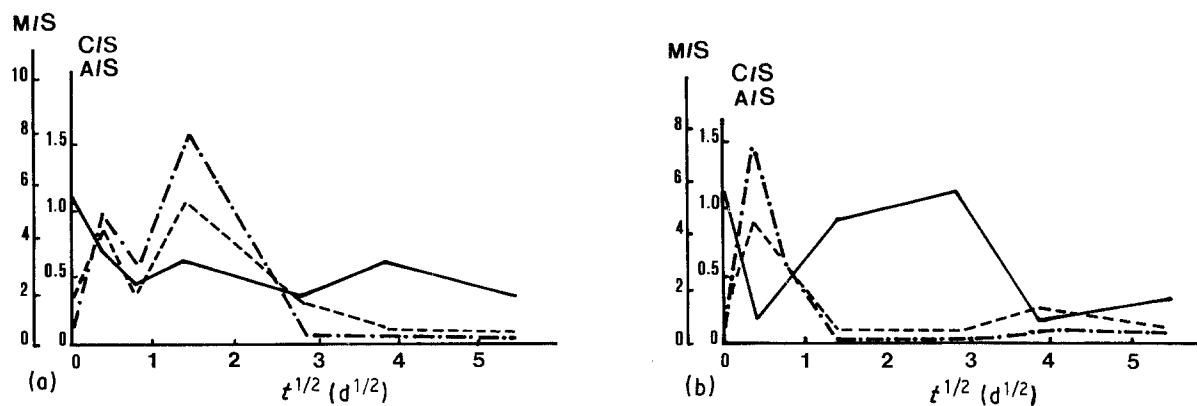
Figure 6 Evolution of L2 slag molar ratios in alkaline media. XPS results in (a) NaOH solution and (b) KOH solution. (—·—) M/S, (——) C/S. (---) A/S.

good agreement with prior XPS data at 2 d, in NaOH solution.

In KOH solution, ultrathin sections for the sample attacked over 2 d (Fig. 8b), also displayed three distinct zones. In spite of similarities of the hydrated glass surface morphologies in NaOH and KOH leachants (SEM data), the EDS results (Table III) indicate distinct compositions in both systems: (i) the scattered lamellae (L) are potassium free and have a similar composition to the hydrated glass substratum (H) on which they grew; (ii) these two previous phases are covered entirely by a lamellar layer (LL), about $0.25 \mu m$ thick, with "silicon-rich-hydrotalcite" composition [20−23], the theoretical pure hydrotalcite being $Mg_6Al_2CO_3(OH)_{16}$, $4H_2O$; (iii) a siliceous layer (S) (0.04 to 0.18 μm) lies upon the former one. No calcium-rich layer was observed in ultrathin sections. Therefore this element, detected by XPS after 2 d, was essentially adsorbed on the outer siliceous layer.

TEM data after long hydration stages (105 and 150 d) are displayed in Figs 8a(i), a(ii) for the hydration in NaOH and Figs 8c and d in KOH. The chemical characterizations by EDS are given in Table IV. From

the unhydrated L1 glass (G), three distinct zones are observed.

(i) an internal granular zone of residual amorphous hydrated glass (H), enriched in silicon, magnesium, aluminium and calcium-poor. After the hydration in NaOH, this layer has concentrated potassium whereas in KOH solution it did not, but accumulated more calcium. At the top are scattered amorphous lamellae (LC) similar in composition;

(ii) an intermediate zone formed by amorphous lamellar layer (LL), enriched in magnesium and aluminium with respect to the lower layer. The composition may be described as corresponding to "silicon-rich hydrotalcite type". Significant potassium contents are found after NaOH attack. In KOH attack, this zone is constituted by several lamellar layers (105 d, Fig. 8c); the chemical composition is less siliceous, without potassium;

(iii) an outer zone. In NaOH attack, it is constituted by a basal granular layer (B), having the same composition to the residual hydrated glass (H), and on which alumino-siliceous particles (AS), and calcium silicate hydrates (CSH) are formed. In KOH solution,

TABLE III L1 glass TEM and EDS analysis on ultrathin sections of samples hydrated in alkaline media (2 d)

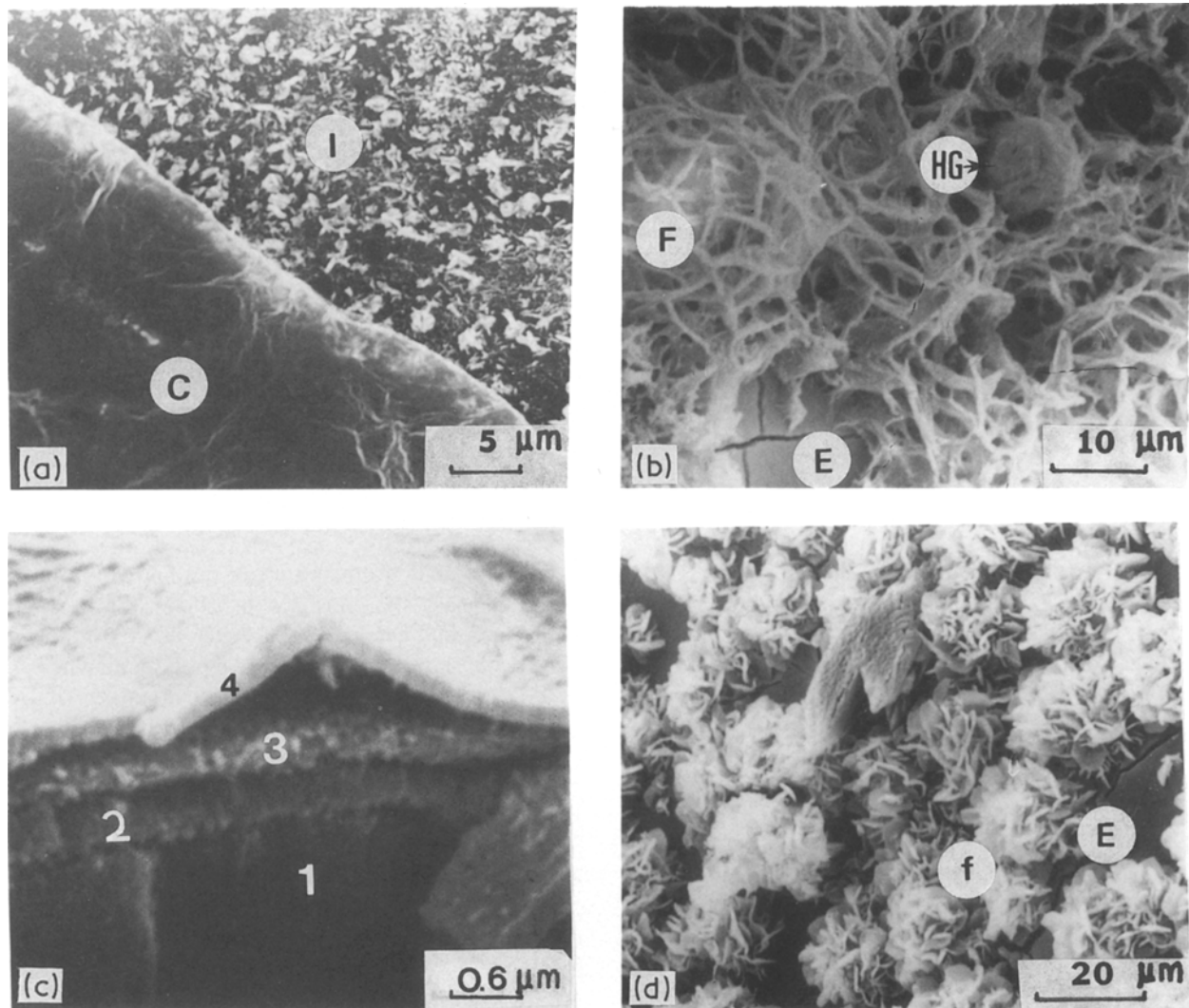| Samples	Chemical composition (wt % oxides)						Morphology
	MgO	Al_2O_3	SiO_2	K_2O	CaO	Fe_2O_3	
L1 NaOH 2 d	–	37	43	–	20	–	Filamentous (C) layer
	–	30	53	16	–	–	Illite (L) lamellae
	–	34	57	–	–	8	Hydrated (H) glass
	4	19	37	–	40	–	Unhydrated (G) glass
L1 KOH 2 d	–	–	+ +	–	–	–	Siliceous (S) layer
(Fig. 8b)	55	20	25	–	–	–	lamellar (LL) layer
	25	20	54	–	–	–	Lamellae (L) Hydrated (H) glass
	8	15	34	–	42	–	Unhydrated (G) glass

+ + = abundant

Figure 7 Surface morphology of L1 slag hydrated in alkaline media (SEM data): in NaOH solution for (a) 2 d, (similar morphology is observed in KOH solution), and (b) 150 d; and in KOH solution after (c) 105 d and (d) 150 d. I = internal layer; C = "crumpled foils" layer; E = granular layer F = "honey-comb" formation; HG = hydrogarnet; 1 = thick layer; 2, 3, 4 = thiner layers; f = flakes.

TABLE IV L1 glass TEM and EDS of ultrathin sections of samples hydrated in alkaline media

| Samples	Chemical composition (wt % oxides)						Morphology
	MgO	Al$_2$O$_3$	SiO$_2$	K$_2$O	CaO	Fe$_2$O$_3$	
L1 NaOH							
150 d	–	9	55	–	34	–	C–S–H
(Figs 8a(i), a(ii))	–	38	54	–	8	–	Particles (AS)
	10	25	51	7	6	–	Basal granular (B) layer
	48	30	17	5	–	–	Amorphous (LL) lamellar layer
	10	25	51	7	6	–	Hydrated (H) glass
	5	20	35	–	40	–	Unhydrated (G) glass
L1 KOH							
105 d	–	–	–	–	+ +	–	Flakes (f)
(Figs. 8c, d)	51	31	11	–	7	–	Amorphous (LL) lamellar layer
	12	26	40	–	21	–	Scattered (LC) lamellae
							Hydrated (H) glass
	5	20	35	–	40	–	Unhydrated (G) glass

+ + = abundant
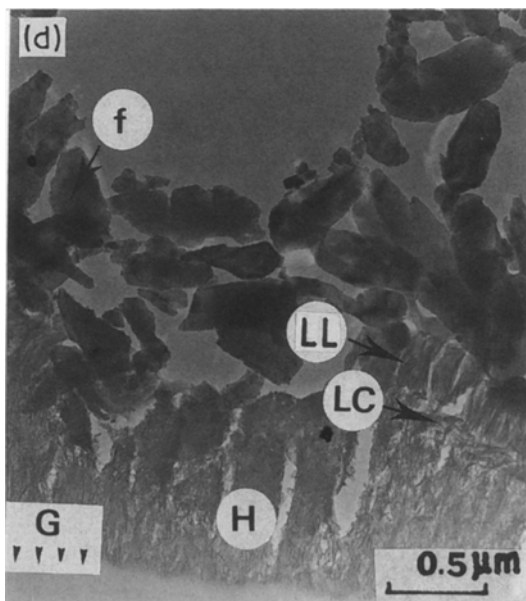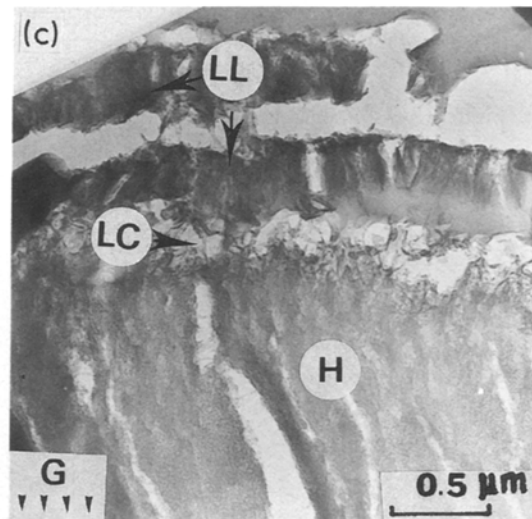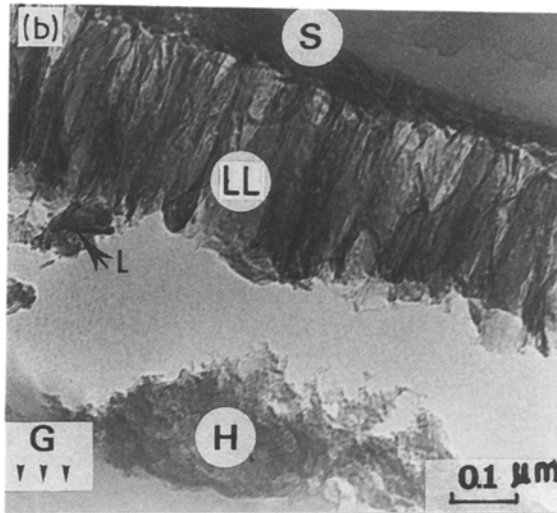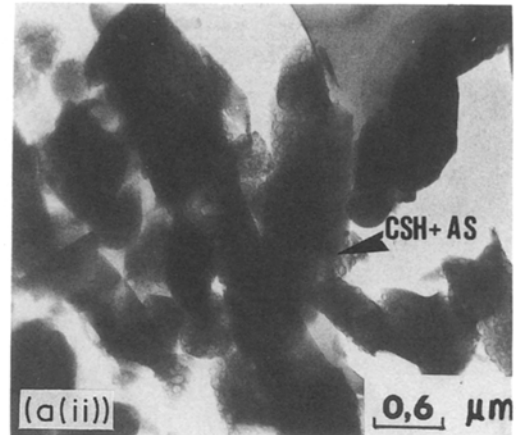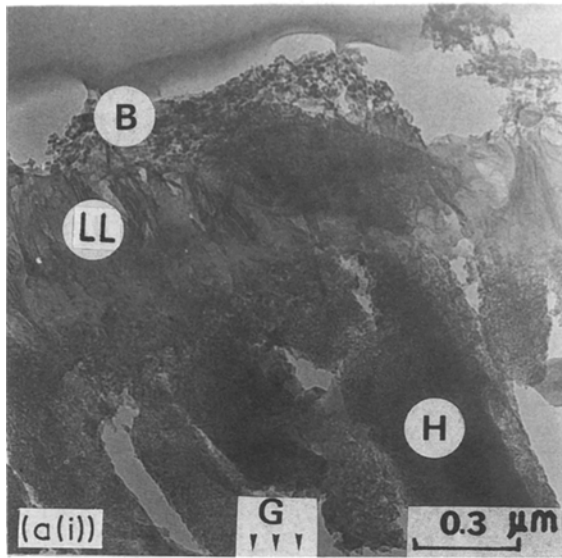
Figure 8 Ultrathin sections of L1 slag hydrated in alkaline media (TEM data) for (a(i)), (a(ii)) 150 d in NaOH solution; (b) 2 d, (c) 105 d and (d) 150 d in KOH solution. G = glass or theoretical position of glass; H = hydrated glass; B = granular layer; LL = lamellar layer; CSH = outer CSH; AS = alumino-siliceous particles; f = calcium containing flakes; S = siliceous layer, LC = internal C–S–H lamellae.

this zone is mostly constituted by unidentified poorly crystallized flakes (F) dominantly calceous in composition.

3.2.3. SEM and TEM data for L2 glass

From SEM observations, after short runs (16 h,

Fig. 9a), a lamellar layer (L) covers the underlying hydrated glass (H). After 2 d (Fig. 9b), the former was coated by an amorphous film (F). Comparing 16 h and 2 d SEM results with XPS analysis, one may suggest that the lamellar layer formed on the hydrated glass is a magnesium, aluminium and silicon containing phase. Unfortunately, we could not obtain ultrathin sections to confirm this assumption. For long-term hydration (150 d) in NaOH medium (Fig. 10a), honey-comb clumps (C), including calcite [12], coated the surface. In KOH solution (Figs 10c and d), the surface morphology involved inner lamellae (L), an intermediate cracked and unstuck layer (E) and outer plates (P).

TEM studies were made on the ultrathin sections cut from the 150 d samples. Identical to L1 glass, three parts are clearly distinguished in the hydrated layer formed on L2 glass surface (Fig. 10b).
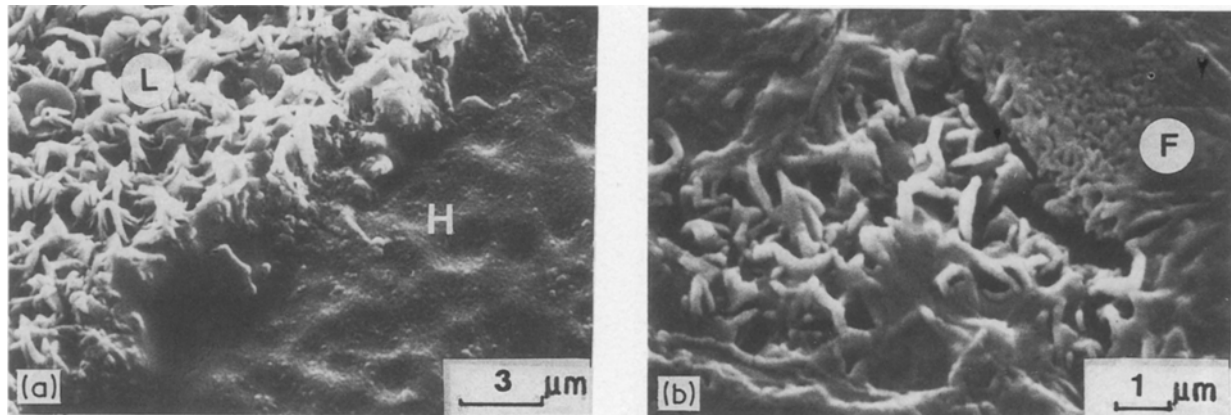
Figure 9 Surface morphology of L2 slag hydrated for short periods in alkaline media: (a) 16 h, (b) 2 d. H = hydrated glass; L = lamellae; F = coating film.

(i) an internal hydrated glass (H);

(ii) an intermediate lamellar layer (LL);

(iii) an outer zone containing a granular formation (g) and thin lamellae (C) (Fig. 10b), or plates (P) (Fig. 10d).

Comparing EDS results (Table V) obtained in the two media, the main points are as follows.

1. In NaOH solution, the residual glass (H) is characterized by an Al–Si–Ca composition; on the contrary, after KOH attack, (H) is magnesian and less enriched in silicon and calcium.

2. The intermediate lamellar layers (LL) have the same chemical composition in both media with significant MgO and Al_2O_3 contents.

3. The outer zone is made of granular formation (g) and aluminosilicates. In NaOH, C–S–H with C/S

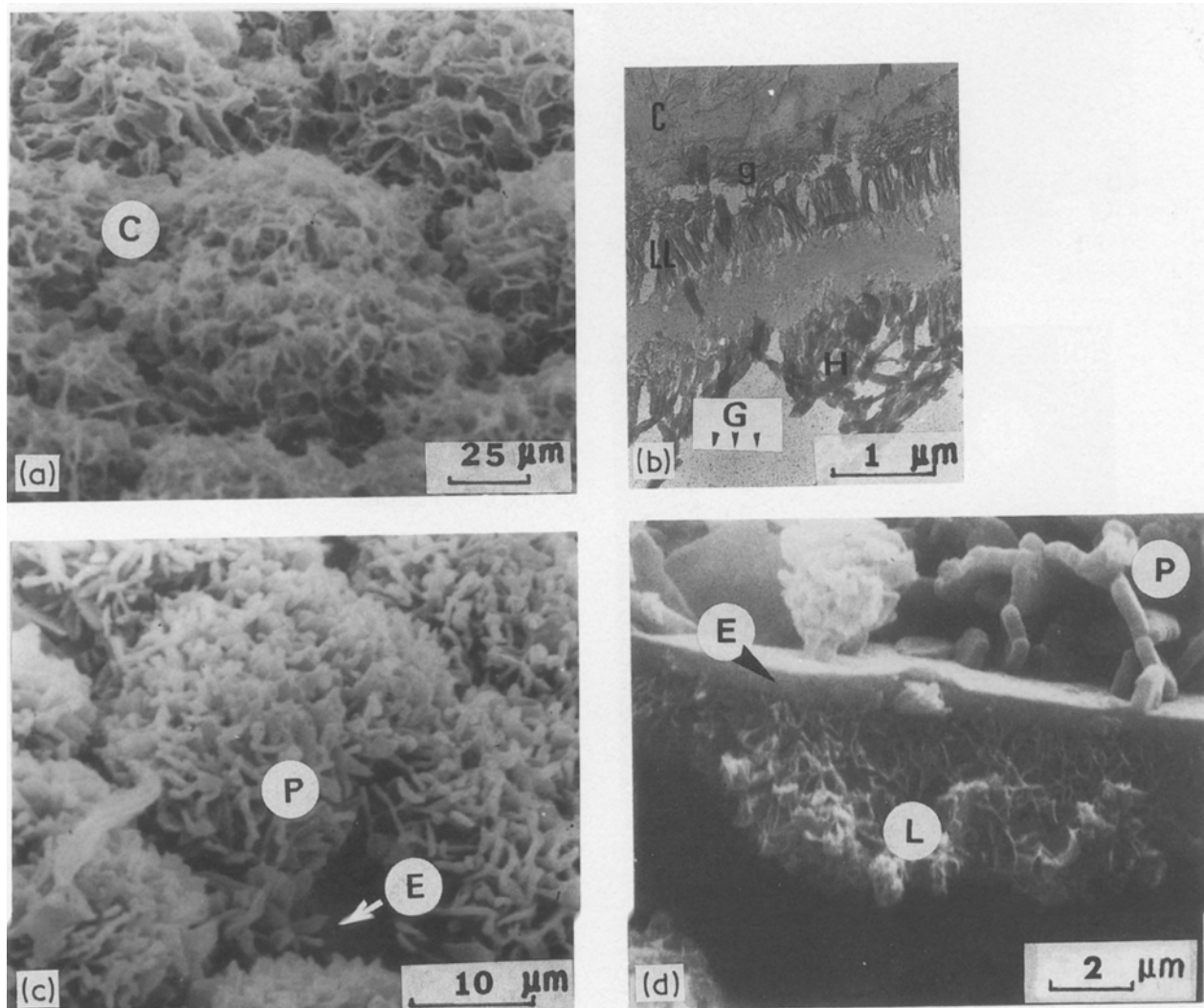*Figure 10* SEM and TEM data for L2 slag hydrated in alkaline media. (a) Surface morphology and (b) ultrathin section for sample hydrated for 150 d in NaOH solution. (c) Surface morphology and (d) structure of different formations for sample hydrated for 150 d in KOH solution. C = honeycomb clumps; g = granular formation; LL = lamellar layer; H = hydrated glass; G = glass; P = plates; E = unstuck layer; L = internal lamellae.

2406

molar ratio ≈ 0.7 and honey-comb aluminosilicates are observed; in KOH, one has C/S molar ratio ≈ 1.4 and plate-like aluminosilicates.

3.2.4. X-ray diffraction results

X-ray analysis on the powder, obtained by scratching the superficial hydrated layer after 150 d reaction gave the following results.

For L1 glass, after NaOH solution attack, hydrated products are constituted by C–S–H, calcite, vaterite, silicocarbonates as scawtite $(Ca_7(Si_6O_{18})\ CO_3H_2O)$, calcium alumino-silicates as gehlenite (C_2ASH) and hibschite $(C_3AS_2H_2)$. After KOH attack C–S–H, scawtite and carbonates (calcite and vaterite) have been found. Contrary to NaOH medium, calcium alumino-silicates are absent. On the other hand, calcium aluminates hydrates C_4AH_x and calcium hydroxide $(Ca(OH)_2)$ have been identified.

For L2 glass, C–S–H, carbonates (calcite) and silicocarbonates (scawtite) have been found. Moreover, after KOH attack C_4AH_x has been determined.

This list is not exhaustive and other species are present [12], including sulphates (e.g. syngenite) whose origin remains obscure, as no sulphur (less than 0.1%S) is present in the slag-like glass composition.

4. Discussion

The above experimental data illustrate the nature and structure of the hydration layers formed on the surface of glassy slags, after different hydration times in different aqueous media. A comprehensive presentation of the results and a preliminary discussion of the effect of alkaline media have been given elsewhere [12, 24].

The discussion will be focused on two points: a synthetic description of the hydrated layers, including a "structural model", and a specific characterization of important secondary phases; a presentation of the mechanisms involved in the glass solution interactions, both in water and in alkaline media and a comparison of the glassy slags L1 and L2.

4.1. Structure and composition of the hydrated layers

From a synthesis of SEM, TEM and XPS data, it is possible to model the structure and composition of the hydrated layers developed in various media.

4.1.1. Hydration in water

The thickness of the hydrated layer is about 0.5 μm after 150 d. There is a rapid formation of a Si–Al residual layer with adsorbed Ca^{2+} and Mg^{2+}; a siliceous veneer appears when silica saturation is reached in the solution and finally, rare amorphous Si–Mg and Si–Al–Mg lamellae scatter on the surface (presumably phyllosilicates growing from the solution).

The chemical differences between the two glassy slags is mostly reflected in the magnesium behaviour; an easier formation of magnesian phases is observed when the more magnesian L2 slag is concerned.
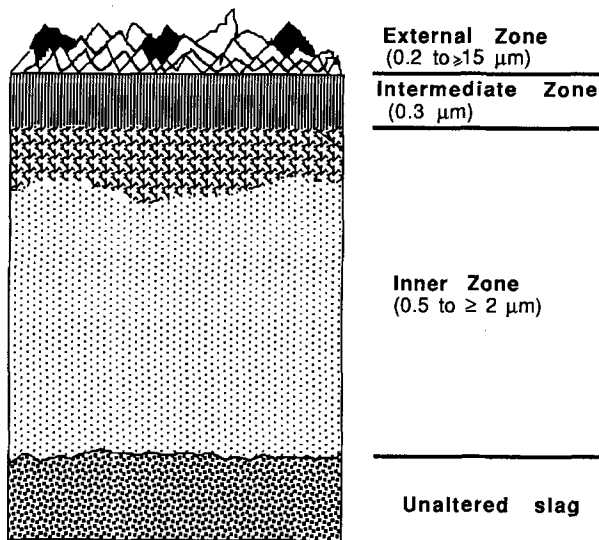
4.1.2. Hydration in alkaline media

4.1.2.1. General structure of the hydrated layers. Glassy slag hydration in alkaline media leads to more complex layers whose detailed descriptions are given elsewhere [12]. Simple structural models (Fig. 11) have been sketched for describing long-term experiments (longer than 30 d). From the unaltered glass to the solution, the following "stratigraphy" is observed:

(i) A complex inner zone, in contact with the glass. Referring to texture, there is a dense residual glass layer, then a lamellar layer with high porosity. The chemical composition is variable, including silicon, aluminium, magnesium as major components, in various proportions with significant calcium. The thickness of this zone is variable with time, 0.5 μm to > 2 μm (150 d).

(ii) An intermediate zone. On the contrary, from 2 d to 150 d, this layer has a constant thickness of about 0.3 μm. It is made of a silicon-bearing "hydrotalcite-type" phase, containing calcium after long runs, and described in the next section.

TABLE V L2 glass TEM and EDS analysis of ultrathin sections of samples hydrated in alkaline media after 150 d

Samples	Chemical composition (wt % oxides)						Morphology
	MgO	Al_2O_3	SiO_2	K_2O	CaO	Fe_2O_3	
L2 NaOH							
150 d	–	38	62	–	–	–	Thin (C) lamellae
(Fig. 10b)							
	–	17	75	–	8	–	Granular (g) layer
	50	27	11	–	12	–	Lamellar (LL) layer
	–	29	60	–	11	–	Hydrated (H) glass
	10	14	36	–	40	–	Unhydrated (G) glass
L2 KOH							
150 d	–	34	66	–	–	–	Plates
	50	26	11	–	13	–	Lamellar (LL) layer
	37	20	37	–	6	–	Hydrated (H) glass
	10	14	36	–	40	–	Unhydrated (G) glass

External Zone
(0.2 to ≥15 μm)

Intermediate Zone
(0.3 μm)

Inner Zone
(0.5 to ≥ 2 μm)

Unaltered slag

☐ Residual hydrated glass

▨ High porosity lamellar layer

Figure 11 Model of the structure of the hydrated layer formed on blast furnace slag after hydration in alkaline media (more than 30 d).

(iii) External zone. This upper part of the profile includes as short term, an Al–Si or Si–rich veneer, lying upon the hydrotalcite-type" phase. Later this zone may enlarge to several micrometers thickness (> 15 μm). The external zone contains a number of crystalline phases.

4.1.2.2. Characterization of "C–S–H types" and "hydrotalcite-type" phases. The development of these phases during L1 and L2 hydration, is described below.

(a) C–S–H type compounds. C–S–H are hydrated calcium silicates with different C/S values and variable aluminium, magnesium and potassium contents [1, 25, 26], in slag hydration. They are important products in hydrated cements and concretes and display a variety of morphologies [12, 27]. Most of these products growing at room temperature are poorly crystallized (plombierite is an exception) or quasi amorphous (tobermoritic gels).

Within ultrathin sections, C–S–H were localized both in the external and internal zones (Fig. 8c). A very large range of C/S values (from 0.4 to 1.4 molar ratios) has been found by EDS analysis as well as variable magnesium, aluminium and potassium contents. Three C–S–H groups may be discriminated

both from their morphology and chemical composition (Fig. 12):

Type 1, the rarest, forms an amorphous gelatinous-like layer, including granules; it has the following composition

$$0.2 < (M + A)/S \text{ (molar ratios)} < 0.6;$$

$$(K + C)/S \text{ (molar ratios)} \leqslant 0.4$$

Type 2, non-crystalline, is plate-shaped and located on the external part of the hydrated layer

$$0.2 < (M + A)/S \text{ (molar ratios)} < 0.5;$$

$$0.6 < (K + C)/S \text{ (molar ratios)} \leqslant 0.9$$

Type 3 has a honeycomb structure and is located both inside and on the external part of the hydrated layer; its chemical composition is as follows

$$A/S \text{ (molar ratios)} < 0.2;$$

$$0.6 \leqslant (K + C)/S \text{ (molar ratios)} < 0.9.$$

This C–S–H is magnesium free. Plombierite, a crystallized C–S–H, (A/S = 0.1 and C/S = 1), has been detected by X-ray diffraction on scratched hydrated powders and electron microdiffraction within ultrathin sections.

The nature of the C–S–H is related both to the glass composition and to the nature of the alkaline medium, as summarized in Table VI. It is noticed that in KOH, both glasses give similar "C–S–H type" compounds. (b) Hydrotalcite type compounds. Hydrotalcite has the general formula [28] $[M_{1-x}R_x(OH)_2]^{+x}$ $[X_{x/n}^{-n}yH_2O]^{-x}$ with M a divalent cation (e.g. Mg^{2+}), R a trivalent one (e.g. Al^{3+}, Fe^{3+}) and X = CO_3^{2-}, OH^- or other anions. Stability is enhanced by high pH.

This compound has been described within cement pastes [1, 23, 29] and may easily fix dissolved silica through rapid adsorption and then through incorporation processes [22]. The Mg–Al–rich phases including silica and calcium (Tables II to V) have been denominated "hydrotalcite type" compounds.

In the hydrated zone, these compounds form a layer of quasi-constant thickness (≈ 0.3 μm) of dense, poorly crystallized thin lamellae. From Tables II to V the mean SiO_2 contents are seen to be about 10% to 15%; it can reach 20% when CaO is undetected in the composition (normalization to 100% of the analysed oxides). From comparisons of ultrathin sections after short- and long-term runs, the genesis of "hydrotalcite type" layer appears resulting from an early process occurring in less than 15 d. XPS data for very short runs suggest the development for the first time of an Al–Si–Mg–rich zone (M/A > 5), rapidly covered by a calcium-rich one. Later, the Mg^{2+} ions, originating

TABLE VI Chemical composition (in molar ratios) of C–S–H in relation to the glass composition and the nature of the alkaline medium

	L1 glass		L2 glass	C–S–H type
NaOH	C/S ≤ 0.8 A/S ≈ 0.4		0.7 ≤ C/S ≤ 1 A/S < 0.2	Type 3
		Mg and K absent		
KOH				Type 2 for
		Mg and K present		outer C–S–H
		0.5 ≤ C/S ≤ 1.4		Type 3 for
		0.2 ≤ A/S ≤ 0.4		inner C–S–H

1.0
0.9
0.8
0.7
0.6
0.5
0.4
0.3

(K+C)/S molar ratios

3

2

1

0   0.1   0.2   0.3   0.4   0.5

(M+A)/S molar ratios

Figure 12 Chemical discrimination between three types of C–S–H from TEM–EDS data.
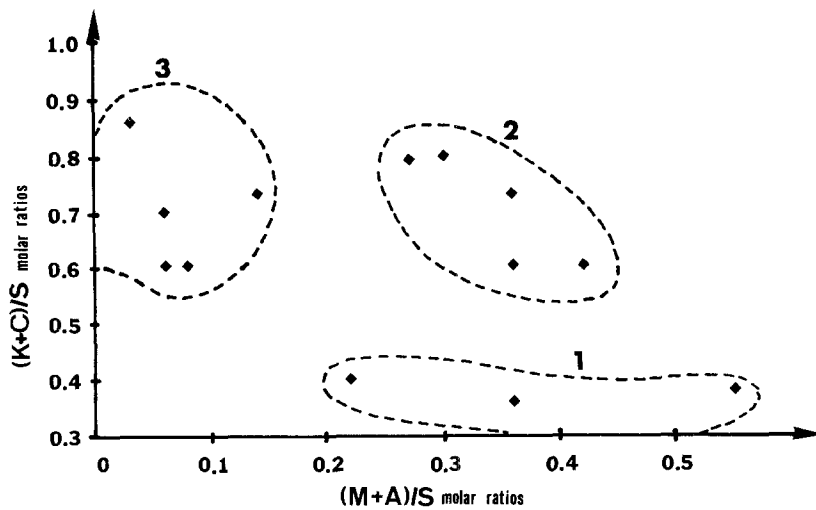
from deep altered glass migrate to the glass surface where they fix OH⁻ [8]. In association with $Al(OH)_4^-$ from the solution, the complex $(AlMg_2) (OH)_6^+$ may form [30], according to the following reaction

$$Al(OH)_4^- + 2[MgOH^+] \rightarrow (AlMg_2)(OH)_6^+$$

Later "hydrotalcite-like" compounds $(3 < M/A < 5)$ may appear, easily fixing amounts of dissolved silica [22] and apparently some calcium.

4.1.3. Comparisons

The higher reactivity of slags in alkaline media is illustrated by the following points: higher thickness of the hydrated layer which is enriched progressively in calcium; higher amounts of C–S–H, with different C–S–H participating in the filling of the pores formed during glass dissolution, and hydrated calcium alumino-silicates; formation of an intermediate layer of "silicon-rich hydrotalcite-type" composition.

On the other hand, some differences have been noted between experiments performed in NaOH and KOH, at the same pH. In particular, a higher calcium and magnesium leaching was noticed in NaOH solutions, resulting in lower calcium and magnesium contents in the hydrated glass (Tables III and V). On the contrary, with KOH solution attack, magnesium-rich hydrated residual glass is formed (Tables III to V).

4.2. Hydration processes
4.2.1. Hydration in water
Resulting from the ion exchange with protons, as classically admitted [31], a calcium and magnesium-depleted surface is rapidly formed. At long times, the hydrated residual Si–Al-rich layer fixes Mg^{2+} from the solution, mostly for the higher magnesian L2 glass. Finally, when the saturation limit is reached in solution, amorphous silica precipitates; this reactive product adsorbs Ca^{2+} but C–S–H growth appears limited.

4.2.2. Hydration in alkaline media
At pH 12.9, the short-term experiments indicate a very rapid glass decalcification. This is explained by the breaking of the Si–O–Si bonds by OH⁻, inducing the formation of a Si–OH bond and enhancing the liberation of modifiers from the glass network. In this

way, a porous hydrated silica-rich frame developed, allowing the aluminium as $(Al(OH)_4^-)$ and magnesium as $(Mg(OH)^+)$ to migrate towards the solution [8]. The higher pH solution prevents any significant solubilization of Mg^{2+} ions adsorbed at the negatively charged surface [32] as $Mg(OH)^+$.

For long-term runs, slag hydration may be described as follows.

(i) Formation of an "hydrotalcite-type" layer at the glass–solution interface resulting from the fixation of $Al(OH)_4^-$ on the magnesium-rich surface layer, forming $(AlMg_2) (OH)_6^+$ and later nucleation and growth of an hydroxycarbonate $(Mg_6Al_2CO_3(OH)_{16} \cdot 4H_2O)$ after fixation of dissolved CO_3^{2-} (from atmospheric CO_2).

(ii) Precipitation of calcite and C–S–H from the solution and simultaneously, fixation of amounts of silica and calcium by the "hydrotalcite-type" phase. For L1 slag glass, (the more aluminous one), calcium alumino-silicate hydrates (gehlenite and hydrogarnets) are formed. For the less aluminous L2 glass, a siliceous veneer precipitates after saturation of the solution with respect to silica.

(iii) Propagation, at depth, of an hydration front leading to the formation of a leached residual glass whose composition will evolve through time by fixation of mobile elements (calcium, magnesium, potassium) "on the way to" or "coming back from" the solution.

5. Conclusions

In order to understand the properties of cement and concrete containing slag powders or sands, one may determine the structure, composition and origin of the hydrated layers grown after different reaction times. In this respect, the results presented in this paper may be summarized as follows.

Two synthetic glassy slags, with high aluminium and magnesium contents, were hydrated at 40°C for 4 h to 150 d, in water and alkaline solutions (NaOH and KOH 0.1 N). After each run, the hydrated zone was characterized using XPS, SEM, TEM of ultra-thin-sections (including EDS analysis) and X-ray diffraction. The composition of the solutions has been given elsewhere [12].

1. In water, the thickness of the hydrated zone is

only about $0.5\,\mu m$ after 150 d. On a silicon- and aluminium-rich leached glass layer, amorphous Si–Mg and Si–Al–Mg lamellae are scattered for the aluminium-rich glass; for the magnesium-rich glass, for long runs, an overlaying lamellar magnesian layer covered by a siliceous veneer was noticed when silica saturation was reached. Ion exchange with protons from the solution, then nucleation and growth of amorphous phases may be involved to explain the origin of the hydrated zone.

2. In alkaline media, short-term experiments (XPS data) indicate a rapid leaching of the glass resulting in the formation of a porous Al–Si-rich layer. Simultaneous migration of aluminium and magnesium from the glass to the solution results in the rapid formation, approximately at the initial solid–solution interface, of a magnesium- and aluminium-rich layer with significant silicon and calcium contents ("hyrotalcite-type" composition). After 15 d, the thickness of this lamellar layer remains constant $(0.3\,\mu m)$.

3. In alkaline media, the hydrated zone is constituted by three distinct parts: an inner residual hydrated glass; an intermediate lamellar layer ("hydrotalcite-type" composition); an outer zone. The intermediate layer separates an inner domain, dominated by the *in situ* formation and evolution of the residual glass, from an outer one, dominated by precipitation process from the solution (e.g. C–S–H and other poorly crystallized calcic phases).

4. Carbonation due to atmospheric CO_2 transformed hydrates to carbonates and silico-carbonates (e.g. scawtite). External layers partly result from the carbonation of former C–S–H [33]. Carbonation being a pseudomorphosis process, the former C–S–H microcrystalline architecture was preserved.

5. The higher reactivity of glassy slags in alkali media, when compared to water, is illustrated by the main following points: the higher thickness of the hydrated zone $(> 20\,\mu m$ at 150 d with respect to $0.5\,\mu m$ in water); precipitation of significant amounts of C–S–H; rapid formation of an Mg–Al-rich layer ("hydrotalcite-type" composition) marking approximately the initial solid–solution interface.

6. Minor differences have been noted between experiments performed in NaOH and KOH as well as between the behaviour of the aluminium-rich and magnesium-rich slag in water and basic media.

References

1. M. REGOURD, in Proceedings of the 7th International Symposium of the Chemistry of Cement, Paris, Vol. 1 (1980) pp. III-2/10.
2. H. TANAKA, Y. TOTANI and Y. SAITO, in Ist International Conference on the use of fly ash, silica fume, slag and other mineral by-products in concrete, Montebello, Canada (1983).
3. M. DAIMON, in Proceedings of the 7th International Symposium of Chemistry of Cement, Paris Vol. II (1980) pp. III-2/1.
4. S. A. ABO- El ENEIN, A. A. ATA, A. HASSANIEN and R. Sh. MIKHAIL, *Sil. Ind.* 6 (1983) 115.
5. R. DRON, Thèse Université Paris VI (1973).
6. *Idem*, in Proceedings of the 7th International Symposium of Chemistry of Cement, Paris, Vol II (1980) pp. 111/134-39.
7. *Idem*, Thèse d'Etat, Université Paris VI (1984).
8. *Idem*, in Proceedings of the 8th Symposium of Chemistry of Cement, Rio de Janeiro, Brazil, Vol. II (1986) pp. 81-85.
9. S. ASANO and M. YANO, *CAJ Rev.* (1982) 51.
10. M. CHERON and C. LARDINOIS, in Proceedings of the 5th International Congress of the Chemistry of Cement, Tokyo, Vol IV (1968) pp. 277-285.
11. Z. RAJAOKARIVONY-ANDRIAMBOLOLONA, Rapport de DEA, Université d'Orléans (1981).
12. *Idem*, Thèse de 3e Cycle Université d'Orléans (1987).
13. M. REGOURD, J. H. THOMASSIN, P. BAILLIF and J. C. TOURAY, *Cem. Conc. Res.* 13 (1983) 549.
14. J. H. THOMASSIN, Thèse de 3e Cycle, Université d'Orléans (1977).
15. M. REGOURD, J. H. THOMASSIN, P. BAILLIF and J. C. TOURAY, in Proceedings of the 7th International Symposium of Chemistry of Cement, Paris Vols I, II (1980) 123/128.
16. J. P. EBERHART and R. TRIKI, *J. Microsc.* 15(2) (1972) 111.
17. E. TADROS, J. SKALNY and S. KALYONCU, *J. Colloid Interface Sci.* 55 (1976) 20.
18. J. H. THOMASSIN, M. REGOURD and P. BAILLIF, *C. R. Acad. Sci.* 228 Série C (1979) 93.
19. I. JAWED, D. MENETRIER, J. SKALNY, in Proceedings of the 7th International Symposium of Chemistry of Cement, Paris, Vol II (1980) pp. 11-182/187.
20. J. H. THOMASSIN, Thèse d'Etat, Université Orléans (1984).
21. J. H. THOMASSIN and J. C. TOURAY, *Bull. Mineral.* 105 (1982) 312.
22. M. GARGOURI, Rapport de DEA, Laboratoire de Cristallographie, Minéralogi et Pétrographie, Université de Strasbourg (1984).
23. G. MASCOLO and O. MARINO, in Proceedings of the 7th International Symposium of Chemistry of Cement, Paris (1980), Vols. II, III-58/62.
24. Z. RAJAOKARIVONY-ANDRIAMBOLONA, J. H. THOMASSIN, P. BAILLIF and J. C. TOURAY, *C. R. Acad. Sci. Paris* 307 Série II (1988) 347.
25. M. REGOURD, B. MORTUREUX, H. HORNAIN and J. VOLANT, in Proceedings of 7th International Symposium of Chemistry of Cement, Paris, Vol. II (1980) III-105/111.
26. R. SERSALE and G. FRIGIONE, *ibid.*, pp. III-63/68.
27. H. F. W. TAYLOR, in Proceedings of the 8th Symposium of Chemistry of Cement, Rio de Janeiro, Brazil, Vol. I (1986) 82-110.
28. G. W. BRINDLEY and G. BROWN (eds), "The X-Ray Identification and Crystal Structure of Clay Minerals" (Mineralogical Society, London) (1963) pp. 361-408.
29. D. M. ROY, E. SONNENTHAL and R. PRAVE, *Cem. Concr. Res.* 15 (1985) 914.
30. H. BESSON, S. CAILLÈRE and S. HENIN, *Bull. Gr. Fr. Argiles* 26 (1974) 79.
31. H. SCHOLTZE, Institut du Verre, Paris (1980).
32. I. TOREANU, M. GEORGESCU and A. PURI, in Proceedings of 7th International Symposium of Chemistry of Cement, Paris (1980) Vols. II, III-99/104.
33. M. MURAT and A. NEGRO, *Matériaux et Construction. Bull. RILEM* 3 (1974) pp. 253-263.